

Furoyl and thiophene carbonyl linker pyrazolyl palladium(II) complexes — Synthesis, characterization, and evaluation as ethylene oligomerization catalysts¹

Stephen O. Ojwach, Mmboneni G. Tshivhase, Ilia A. Guzei, James Darkwa, and Selwyn F. Mapolie

Abstract: Reactions of 2-furoyl chloride and 2-thiophene carbonyl chloride with substituted pyrazoles produced the modified pyrazolyl compounds: {(3,5-Me₂pzCO)-2-C₄H₃O} (**L1**), {(3,5-Me₂pzCO)-2-C₄H₃S} (**L2**), {(3,5-*t*-Bu₂pzCO)-2-C₄H₃O} (**L3**), {(3,5-*t*-Bu₂pzCO)-2-C₄H₃S} (**L4**), {(3,5-Ph₂pzCO)-2-C₄H₃S} (**L5**), and {(pzCO)-2-C₄H₃O} (**L6**) in good yields. Reactions of these synthons with [Pd(NCMe)₂Cl₂] afforded the corresponding mononuclear palladium(II) complexes: [Pd(**L1**)₂Cl₂] (**1**), [Pd(**L2**)₂Cl₂] (**2**), [Pd(**L3**)₂Cl₂] (**3**), [Pd(**L4**)₂Cl₂] (**4**), [Pd(**L5**)₂Cl₂] (**5**), and [Pd(**L6**)₂Cl₂] (**6**) in moderate to high yields. All compounds synthesized were characterized by a combination of ¹H NMR, ¹³C NMR, and IR spectroscopy. Compounds **L1**, **1**, and **2** were examined by single crystal X-ray crystallography. DFT theoretical studies at the B3LYP/6-31+G(*d*) level of theory with GAUSSIAN98 have been used to rationalize some of the results. When the complexes were activated with ethylaluminium dichloride (EtAlCl₂), they catalysed the oligomerization of ethylene to mostly C₁₀ and C₁₂ oligomers. Oligomer distribution greatly depends on the oligomerization conditions; for example, an increase in temperature and pressure produced a higher percentage of C₁₂ compared to C₁₀.

Key words: furoyl and thiophene carbonyl linker pyrazolyl compounds, palladium complexes, ethylene oligomerization.

Résumé : Les réactions du chlorure de 2-furoyle et le chlorure de thiophène-2-carbonyle avec des pyrazoles substitués conduisent avec de bons rendements aux composés pyrazolyles modifiés: {(3,5-Me₂pzCO)-2-C₄H₃O} (**L1**), {(3,5-Me₂pzCO)-2-C₄H₃S} (**L2**), {(3,5-*t*-Bu₂pzCO)-2-C₄H₃O} (**L3**), {(3,5-*t*-Bu₂pzCO)-2-C₄H₃S} (**L4**), {(3,5-Ph₂pzCO)-2-C₄H₃S} (**L5**) et {(pzCO)-2-C₄H₃O} (**L6**). Les réactions de ces synthons avec du [Pd(NCMe)₂Cl₂] conduisent avec des rendements allant de modérés à élevés aux complexes mononucléaires correspondants du palladium(II): [Pd(**L1**)₂Cl₂] (**1**), [Pd(**L2**)₂Cl₂] (**2**), [Pd(**L3**)₂Cl₂] (**3**), [Pd(**L4**)₂Cl₂] (**4**), [Pd(**L5**)₂Cl₂] (**5**) et [Pd(**L6**)₂Cl₂] (**6**). Tous les composés synthésés ont été caractérisés par une combinaison de spectroscopie infrarouge et RMN du ¹H et du ¹³C. Les composés **L1**, **1** et **2** ont été examinés par diffraction des rayons X. Des études selon la théorie de la densité fonctionnelle au niveau B3LYP/6-31+G(*d*) de la théorie avec une GAUSSIAN98 ont été utilisées pour rationaliser un certain nombre de résultats. Lorsqu'ils sont activés par du dichlorure d'éthylaluminium (EtAlCl₂), ils catalysent l'oligomérisation de l'éthylène, principalement en oligomères en C₁₀ et en C₁₂. La distribution des oligomères dépend fortement des conditions d'oligomérisation; par exemple, une augmentation de la température et de la pression conduit à des pourcentages plus élevés de produit en C₁₂ par rapport à celui en C₁₀.

Mots clés : furoyle et thiophène carbonyle, lieu, composés pyrazolyles, complexes du palladium, oligomérisation de l'éthylène.

[Traduit par la Rédaction]

Introduction

Nitrogen donor compounds represent an important class of ligands in coordination chemistry. In particular, pyrazoles and pyrazolyl ligands have been widely used as terminal and bridging ligands and as precursors for various multidentate

ligands in coordination chemistry (1). Indeed, the chemistry of pyrazole and pyrazolyl complexes with transition metals has been extensively reviewed (2), but despite the numerous reports on the synthesis and properties of pyrazolyl late transition metal complexes, very little is known about their catalytic activity in olefin oligomerization. Olefin oligomeri-

Received 9 December 2004. Published on the NRC Research Press Web site at <http://canjchem.nrc.ca> on 22 July 2005.

S.O. Ojwach, M.G. Tshivhase, J. Darkwa,² and S.F. Mapolie.³ Department of Chemistry, University of the Western Cape, Private Bag X17, Bellville 7535, South Africa.

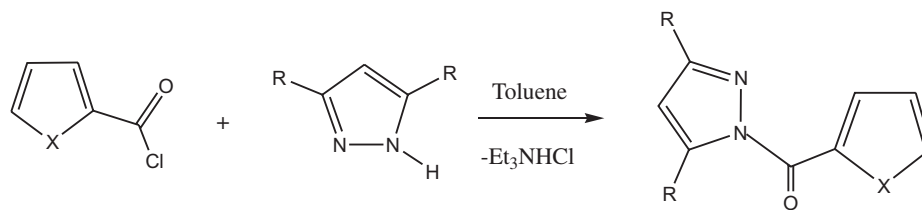
I.A. Guzei. Department of Chemistry, University of Wisconsin-Madison, 1101 University Avenue, Madison, WI 53706, USA.

¹This article is part of a Special Issue dedicated to Professor Howard Alper.

²Corresponding author (e-mail: jdarkwa@uwc.ac.za).

³Corresponding author (e-mail: smapolie@uwc.ac.za).

Scheme 1.



Compound	X	R	Compound	X	R
L1	O	Me	L4	S	^t Bu
L2	S	Me	L5	S	Ph
L3	O	^t Bu	L6	O	H

zation is typically catalysed by late transition metal complexes, particularly those of Ni(II) with P, N, and O ligands (3) because of the propensity of such reactions to undergo β -hydride elimination.

However, in the last decade it has become clear that careful tuning of ligand properties and choice of appropriate co-catalysts can lead to either oligomers or polymers after this phenomenon was first observed by Keim (4). For example, reports by Brookhart and co-workers (5) clearly demonstrate the effect of bulky substituents in pseudo axial sites in nickel catalysts. Bulky ligands block these axial sites and reduce chain transfer, whereas less bulky ligands form catalysts that produce oligomers. Another example of the role of bulky substituents on catalysts is provided by diimine-pyridine ligands. Gibson and co-workers (6) have used Fe(II) and Co(II) complexes of this ligand system, with bulky ligands, as catalysts to polymerize ethylene. However, by reducing the steric bulk of the ligand backbone, the Brookhart group found the Fe(II) catalyst to oligomerize ethylene to linear α -olefins with remarkable activity and selectivity (7).

Recently, pyrazolyl nitrogen donor ligands have been found to be tunable to produce electronic and steric effects that have resulted in the use of their late transition metal complexes as catalysts for the transformation of unsaturated hydrocarbons. The report on the polymerization of ethylene by $[\{R_2C(3-t-Bu_2pz)_2\}PdCl_2]$ (R = Me, Ph) represents one of the first examples of the use of pyrazolyl late-transition metal complexes in olefin polymerization catalysis (8). Reports by our group clearly indicate that electrophilicity of the catalyst plays a crucial role in polymer formation. We have found simple pyrazole Ni(II) and Pd(II) complexes that are good catalysts for ethylene polymerization (9), and by introducing carbonyl linkers to form benzenedicarbonyl and benzenetricarbonyl linker pyrazolyl palladium(II) complexes, catalytic activities for ethylene polymerization are significantly higher than for the analogous simple pyrazole systems (10). Steric factors also play a role (11). Our calculations of the steric encumbrance about the central metals indicate that in complex $[(3,5-t-Bu_2pz)_2PdCl_2]$ the ligands shield 92.1(3)% of the Pd surface while in $[(3,5-Mepz)_2PdCl_2]$ only 83.5(6)% of the central Pd is shielded by the coordinated moieties (12). In producing polyethylene,

we have used mainly methylaluminoxane (MAO), but generally ethylaluminum halides can also activate precatalysts to polymerize ethylene (3).

In this report we describe the preparation and characterization of new furoyl and thiophene carbonyl Pd(II) complexes and their ability to catalyze ethylene oligomerization when activated by ethylaluminum dichloride ($EtAlCl_2$) as the co-catalyst. The potential for controlling the catalytic properties by varying substituents on the ligands is demonstrated by using different substituted pyrazolyl compounds. The influence of various conditions such as reaction time and temperature on the catalyst activity and selectivity in ethylene oligomerization is described.

Results and discussion

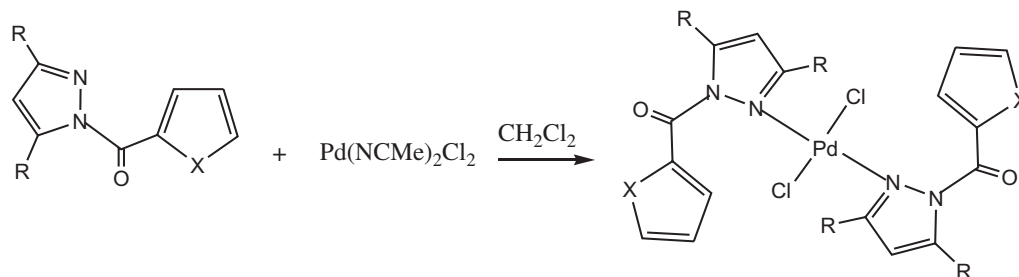
Synthesis and characterization of 2-furoyl and thiophene carbonyl pyrazolyl compounds and their palladium(II) complexes

The compounds **L1–L6** were readily prepared from either 2-furoyl chloride or 2-thiophene carbonyl chloride and an equivalent amount of the appropriate pyrazole (Scheme 1) following the procedure previously described by us (10). The yields were moderate to high (53%–85%).

Reactions of **L1–L6** with $[Pd(NCMe)_2Cl_2]$ in a 2:1 ratio produced the corresponding complexes **1–6** (Scheme 2). While **1–5** were soluble in dichloromethane and could be purified by recrystallization from dichloromethane and hexane (1:1), **6** was insoluble in common organic solvents like dichloromethane, toluene, and acetonitrile. Complex **6** precipitated from the reaction mixture essentially as an analytically pure solid.

All compounds were characterized by a combination of IR, 1H NMR, and ^{13}C NMR spectroscopy and elemental analyses. Structures for **L1**, **1**, and **2** were confirmed by X-ray crystallography. 1H NMR spectroscopy, however, offered signals that allowed easy identification of both ligands and complexes. For example, the 3,5-disubstituted alkyl pyrazolyl compounds typically have two upfield signals for the alkyl substituents, a signal at about 6 ppm and three doublets of doublets with an AMX splitting pattern (13). As expected, the heteroatom in the linker affected the chemical shift, par-

Scheme 2.



Complex	X	R	Complex	X	R
1	O	Me	4	S	^t Bu
2	S	Me	5	S	Ph
3	O	^t Bu	6	O	H

ticularly those close to these atoms. Complexation of pyrazolyl compounds with Pd resulted in slight changes of the ligands NMR chemical shifts, but there were essentially no changes in the signals in the splitting patterns.

Molecular structure determination by single crystal X-ray analysis

Single crystals suitable for X-ray analysis for compound **L1**, complexes **1** and **2** were grown by slow diffusion of hexane into dichloromethane at $-4\text{ }^{\circ}\text{C}$ and used to determine their molecular structures. Crystallographic data for **L1**, **1**, and **2** are presented in Table 1 while selected bond distances and angles are tabulated in Tables 2–4, respectively. The molecular diagrams are presented in Figs. 1–3, respectively.

The solid-state conformation of **L1** is consistent with the results of the DFT studies (vide infra) of its simplified analogue pz-C(O)-C₄H₃O. In the structure of **L1**, atoms N(1) and O(1) are on the opposite sides of the N(2)—C(6) bond owing to electrostatic interactions (14) and atoms O(1) and O(2) are on the same side of the C(6)—C(7) bond. This spatial arrangement is also observed in the structure of **1**, revealing that the preferred orientation is not altered upon coordination.

The two palladium complexes **1** and **2** contain the central metal in slightly distorted square-planar arrangements. In both cases, the pyrazolyl ligands are trans to each other rendering *C_i* molecular symmetry. This is in line with our density functional theory studies of *trans*-(pzH)₂PdCl₂ (symmetry *C_{2h}*) and *cis*-(pzH)₂PdCl₂ (symmetry *C₂*) at the B3LYP/LANL2DZ level of theory that indicate that the *trans*-complex is 12.82 kcal mol⁻¹ (1 cal = 4.184 J) more stable. Compounds **L1** and **L2** are not planar in their respective complexes and are monodentate with the heteroatoms sulfur and oxygen pointing away from the metal centres.

The average Pd—N bond lengths of 2.032(2) and 2.025(7) Å in complexes **1** and **2**, respectively, are statistically indistinguishable and agree well with the average Pd—N(pz) bond length of 2.06(9) Å determined by averaging

607 bonds in 229 relevant complexes reported to the Cambridge Structural Database (CSD, (15)). The Pd—Cl bond distances in **1** and **2** (2.306(9) and 2.306(3) Å, respectively) are in good agreement with the distance of 2.33(5) Å obtained by averaging 2055 Pd—Cl bonds in 1268 relevant complexes reported to the CSD.

An interesting structural aspect was revealed by examining the ligand conformations in complexes **1** and **2**. The ligands differ only by the nature of the heteroatom (sulfur vs. oxygen) in their non-pyrazole five-membered rings and one could have reasonably expected to observe very similar structures. Indeed, in both cases the heteroatom (S or O) is located on the same side of the C—C bond of the X-C-C=O link in each ligand. Recall that in free **L1** (Fig. 1), the two oxygen atoms reside on the same side of the O-C-C=O linkage. This logical result is in line with expectations, however, DFT theoretical studies of simplified analogues of the compounds **L1** and **L2** (Figs. 4 and 5) at the B3LYP/6-31+G(*d*) level of theory with GAUSSIAN98 (16) indicate that a different outcome could have been predicted. The compounds (**L1** and **L2**) can exist in several stable conformations; the two most stable are shown in Figs. 4 and 5. In the case of furoyl, the conformation in which the furan oxygen is positioned on the same side as the carbonyl oxygen in the O-C-C=O sequence is more stable. This conformation (A in Fig. 4) is observed in the crystal structures of both **L1** and **1**. On the other hand, in the case of the thiophene carbonyl compound, the other conformation (D in Fig. 5), in which the thiophene S atom is on the opposite side from the carbonyl ligand in the S-C-C=O sequence is slightly more stable. Thus, the free compound **L2** changes its conformation upon coordinating to the Pd metal centre during the formation of **2**. The activation energies for the rotation about the C—C bond of the X-C-C=O linkage are calculated to be 13.4 kcal mol⁻¹ for the A to B and 7.1 kcal/mol for C to D transitions.

We have also examined the steric crowding around the Pd centres in **1** and **2** with the program SOLID-G to determine

Table 1. Crystal data and details of structure refinement for **L1**, **1**, and **2**.

Parameter	L1	1	2
Empirical formula	C ₁₀ H ₁₀ N ₂ O ₂	C ₂₀ H ₂₀ Cl ₂ N ₄ O ₄ Pd	C ₂₁ H ₂₂ Cl ₄ N ₄ O ₂ PdS ₂
Formula weight	190.2	557.7	674.75
Temperature (K)	294(2)	273(2)	100(2)
Wavelength (Å)	0.710 73	0.710 73	0.710 73
Crystal system	Monoclinic	Triclinic	Monoclinic
Space group	<i>P</i> 2 ₁ / <i>n</i>	<i>P</i> $\bar{1}$	<i>P</i> 2 ₁
<i>a</i> (Å)	8.005 7(10)	7.442 2(8)	10.696(2)
<i>b</i> (Å)	17.761(2)	9.209 7(10)	13.332(3)
<i>c</i> (Å)	13.808 3(15)	15.742 2(17)	18.015(4)
α (°)	90	88.898(2)	90
β (°)	97.148(2)	88.049(2)	96.345(4)
γ (°)	90	86.608(2)	90
Volume (Å ³)	1948.2(4)	1948.2(4)	2553.1(9)
<i>Z</i>	8	2	4
Density (calculated, Mg m ⁻³)	1.297	1.721	1.755
Absorption coefficient (mm ⁻¹)	0.093	1.146	1.337
<i>F</i> (000)	800	560	1352
Crystal size (mm ³)	0.40 × 0.20 × 0.10	0.43 × 0.32 × 0.26	0.30 × 0.20 × 0.20
θ Range for data collection (°)	1.88–26.38	2.22–26.39	1.90–28.31
Index ranges	–10 ≤ <i>h</i> ≤ 9, –22 ≤ <i>k</i> ≤ 20, –16 ≤ <i>l</i> ≤ 7	–9 ≤ <i>h</i> ≤ 9, –11 ≤ <i>k</i> ≤ 11, –19 ≤ <i>l</i> ≤ 19	–14 ≤ <i>h</i> ≤ 12, –16 ≤ <i>k</i> ≤ 17, –23 ≤ <i>l</i> ≤ 20
Reflections collected	9077	8891	16 039
Independent collections	3753 (<i>R</i> (int) = 0.029 6)	4401 (<i>R</i> (int) = 0.020 7)	10 824 (<i>R</i> (int) = 0.051 2)
Completeness to θ (%)	94.2	99.1	92.8
Absorption corrections	Empirical with SADABS	Empirical with SADABS	Empirical with SADABS
Max and min transmissions	0.990 8 and 0.963 9	0.754 9 and 0.638 6	0.754 9 and 0.638 6
Refinement method	Full-matrix least-squares on <i>F</i> ²	Full-matrix least-squares on <i>F</i> ²	Full-matrix least-squares on <i>F</i> ²
Data/restraints/parameters	3753/0/313	4401/0/287	10 829/409/622
Goodness of fit on <i>F</i> ²	1.025	1.063	1.045
Final <i>R</i> indices	<i>R</i> 1 = 0.051 3, <i>wR</i> 2 = 0.126 4	<i>R</i> 1 = 0.027 1, <i>wR</i> 2 = 0.073 7	<i>R</i> 1 = 0.061 2, <i>wR</i> 2 = 0.139 9
<i>R</i> indices (all data)	<i>R</i> 1 = 0.094 8, <i>wR</i> 2 = 0.145 7	<i>R</i> 1 = 0.028 8, <i>wR</i> 2 = 0.075 0	<i>R</i> 1 = 0.069 6, <i>wR</i> 2 = 0.147 9
Largest diff. peak and hole (e Å ⁻³)	0.174 and –0.245	1.011 and –0.529	3.060 and –0.849

that the metal centres are shielded by the ligands to the extent of 93.1(3)% and 92.3(5)%, respectively. Since the difference between these values, determined from the crystal structures reported herein, is not statistically significant, any variation in the reactivity of these complexes towards the same reagents ought to be attributed to the differences in the electronic properties of the ligands and their conformations.

Evaluation of the complexes as catalysts for ethylene oligomerization

When complexes **1–5** were activated with EtAlCl₂, they were found to oligomerize ethylene to mainly C₁₀ and C₁₂. No oligomers were obtained when controlled reactions were carried out at 25 °C and 5 atm (1 atm = 101.325 kPa) with the co-catalyst and ethylene in the absence of the complexes. Complex **6** was not evaluated because it is insoluble in toluene, the oligomerization solvent. There were a number of factors that influenced the oligomerization: First, the nature of the ligands influenced both the catalyst activity and product distribution. Complex **1**, with the fuoyl linker and methyl groups, was less active (TON = 60 kg mol⁻¹ Pd h⁻¹)

than the analogous complex **3** with *tert*-butyl substituents (TON = 70 kg mol⁻¹ Pd h⁻¹) (Table 5, entries 1 and 3). A similar trend was observed for the thiophene carbonyl analogue (Table 5, entries 2 and 5). Catalyst **5**, with the phenyl substituent on the pyrazolyl ring, was the most active.

A report by Guan and Marshall (17) on the catalytic behaviour of phosphine–imine Pd(II) complexes shows that the phenyl analogue has higher activity (TON = 17 200 kg mol⁻¹ Pd h⁻¹) compared to that of the *tert*-butyl (TON = 1670 kg mol⁻¹ Pd h⁻¹) and the methyl (TON = 960 kg mol⁻¹ Pd h⁻¹) systems. The observed trend could be ascribed to the difference in the electronic structure of the complexes (18) where the less electron-donating phenyl group produces a more electrophilic metal centre in the catalyst. This could explain why complex **5** is the best catalyst in our study.

The nature of the linker in the ligand systems appears to have some effect on the oligomer distribution. For example, the catalysts with fuoyl linkers gave higher percentages of the C₁₂ than C₁₀ oligomers (Table 5, entries 1 and 3) whereas the thiophene carbonyl analogues gave higher percentages of

Table 2. Selected bond lengths and angles for **L1**.

Bond lengths (Å)	
O(1)—C(6)	1.209(2)
O(2)—C(10)	1.355(3)
O(2)—C(7)	1.377(2)
N(1)—C(2)	1.311(3)
N(1)—N(2)	1.379(2)
N(2)—C(6)	1.405(2)
Bond angles (°)	
C(10)—O(2)—C(7)	105.82(18)
N(1)—N(2)—C(4)	111.88(16)
N(1)—N(2)—C(6)	120.58(16)
O(2)—C(7)—C(6)	112.40(17)
O(1)—C(6)—C(7)	122.49(18)
N(2)—C(6)—C(7)	117.53(17)

Table 3. Selected bond lengths and angles for **1**.

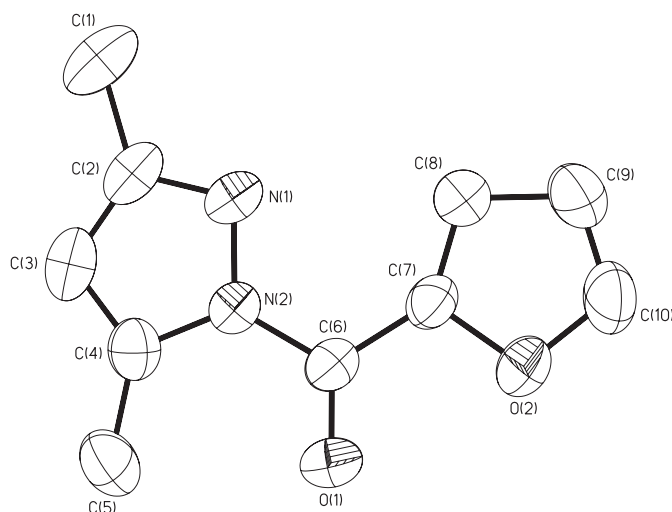
Bond lengths (Å)	
Pd(1)—N(1)	2.0332(15)
Pd(1)—Cl(1)	2.2993(5)
Pd(2)—N(3)	2.0300(17)
Pd(2)—Cl(2)	2.3125(5)
N(1)—C(2)	1.327(2)
N(1)—N(2)	1.388(2)
O(1)—C(6)	1.203(2)
Bond angles (°)	
N(1)—Pd(1)—N(1)	180.00(8)
N(1)—Pd(1)—Cl(1)	91.84(5)
N(1)—Pd(1)—Cl(1)	88.16(5)
N(1)—Pd(1)—Cl(1)	91.84
N(3)—Pd(2)—Cl(2)	88.84(5)
N(3)—Pd(2)—Cl(2)	91.16(5)
N(2)—C(6)—C(7)	116.36(16)

C₁₀ than C₁₂ (Table 5, entries 2 and 4). There was, however, no clear trend in oligomer distribution as the steric bulk of the ligands in the catalysts changed.

The co-catalyst to catalyst ratio was found to be crucial in determining activity. Complex **2** was used to establish the effective ratio for optimum activity. No activity was observed for an Al:Pd ratio below 20. This indicates that not much activation occurs below this ratio. An increase in the Al:Pd from 20 to 2000 resulted in a general increase in oligomer yield to give an optimum ratio of 1000. Above this ratio, the yield decreased (Table 6, entry 6). Catalyst **1** showed a similar trend (Table 6, entries 7–9). The co-catalyst to catalyst ratio in ethylene oligomerization catalysed by phosphinitooxazoline and pyridine Ni(II) complexes is known to increase turnover frequency from 11 600 to 49 000 mol C₂H₄ mol⁻¹ Ni h⁻¹ when the EtAlCl₂:Ni ratio is increased from 1.3 to 6 (19). Our catalyst requires much higher co-catalyst to catalyst ratio. This is probably due to the ability of the co-catalyst to interact with both the carbonyl oxygen and the heteroatom in the ligands. We found a higher Al:Pd ratio, however, resulted in an increase in the percentage of C₁₀ oligomers. For instance, an Al:Pd of 50 gave 49% of C₁₀ and 45% of C₁₂,

Table 4. Selected bond lengths and angles for **2**.

Bond lengths (Å)	
Pd(1)—N(1A)	2.026(6)
Pd(1)—Cl(1)	2.3029(19)
Pd(2)—N(1B)	2.035(6)
Pd(1)—Cl(2)	2.3101(19)
S(14A)—C(13A)	1.694(8)
O(9A)—C(8A)	1.202(8)
N(1A)—C(2A)	1.363(8)
Bond angles (°)	
N(1A)—Pd(1)—N(1B)	178.7(3)
N(1A)—Pd(1)—Cl(1)	88.47(5)
N(1B)—Pd(1)—Cl(1)	90.93(5)
N(1A)—Pd(1)—Cl(2)	91.29(17)
N(1C)—Pd(2)—N(1D)	179.5(3)
O(9A)—C(8A)—N(7A)	119.5(7)
O(9A)—C(8A)—C(10A)	123.4(7)

Fig. 1. ORTEP diagram of a single moiety of **L1**. Atoms are shown with 50% thermal probability ellipsoids.

while an Al:Pd of 1000 gave 66% C₁₀ and 30% C₁₂. It is not clear why the changes in co-catalyst to catalyst ratio affect product distribution.

The effects of time, temperature, and pressure on ethylene oligomerization were mainly investigated using catalysts **1** and **5**. The effect of time on ethylene oligomerization activity using catalyst **1** at 25 °C, 5 atm, and an Al:Pd ratio of 500 was investigated. Longer reaction times resulted in a significant decrease in activity (Table 7). The maximum turnover number (177 kg mol⁻¹ Pd h⁻¹) was obtained at 30 min (Table 7, entry 2), but at 15 min, it was evident that the process to produce the active species was still incomplete, resulting in lower yields (120 kg mol⁻¹ Pd h⁻¹). The same trend was observed for catalyst **5** (Table 7, entries 5 and 6). Generally, reaction time is known to affect catalyst activity. This is usually the result of catalyst decomposition. Our catalysts appear to be stable up to about 30 min and thereafter begin to decompose, even at room temperature. A similar phenomenon is seen for ethylene oligomerization using cationic Ni(II) and Pd(II) complexes containing bidentate phen-

Fig. 2. ORTEP diagram of **1** shown with 50% probability ellipsoids. The hydrogen atoms are omitted for clarity. The complex resides on a crystallographic inversion centre.

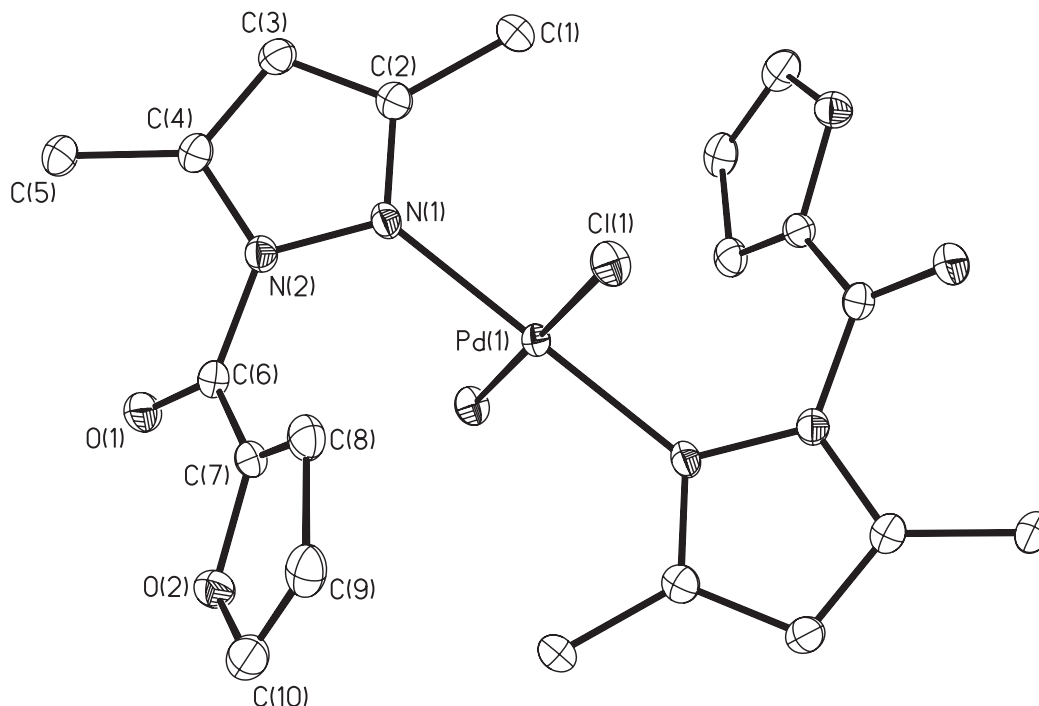
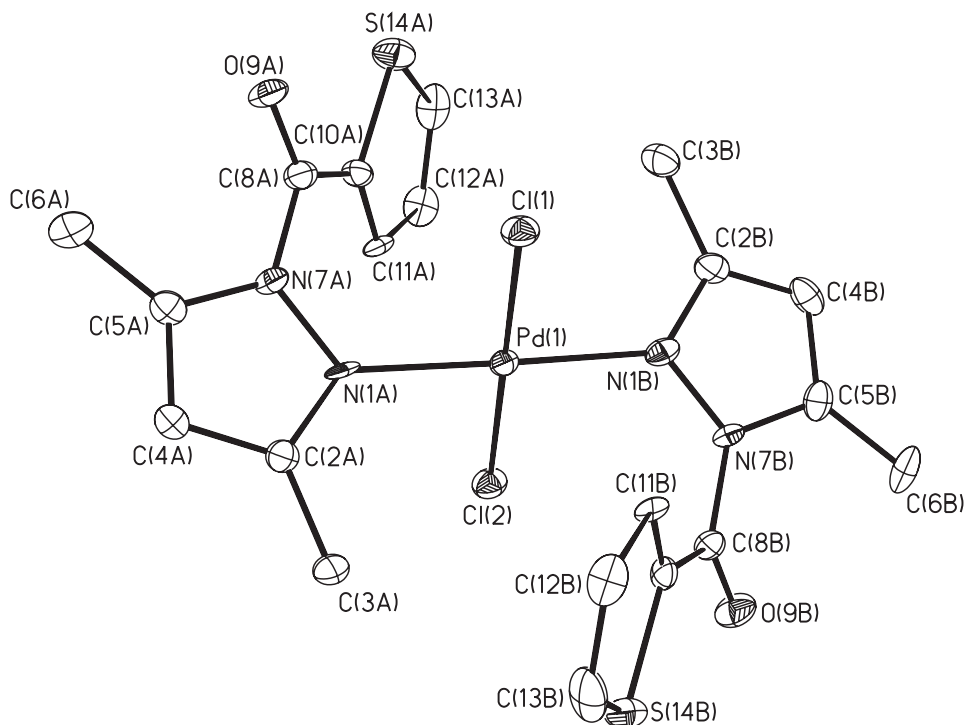


Fig. 3. ORTEP diagram of **2** drawn with 50% thermal probability ellipsoids. The hydrogen atoms have been omitted for clarity.



acyldiarylphosphine ligands (**20**), where TOF increases for the Pd(II) catalyst from $1.2 \times 10^3 \text{ h}^{-1}$ in 15 min to $5.3 \times 10^4 \text{ h}^{-1}$ of ethylene consumed in 1 h, but after 3 h of activity dropped to $3.3 \times 10^4 \text{ h}^{-1}$, signifying some catalyst decomposition.

Reaction time was also found to have a profound effect on

the nature of the oligomers produced. A higher percentage of C_{10} (77%) was obtained for the 15 min run as compared to 38% for the 2 h run (Table 7, entries 1 and 4). This indicates that oligomer molecular weight increases with time, a result of co-oligomerization of the released matured oligomers, hence, production of higher oligomers. An opposite

Table 5. Effect of the catalyst on ethylene oligomerization.^a

Entry	Catalyst	Oligomers (%) ^b			Yield ^c (g)	TON (kg mol ⁻¹ Pd h ⁻¹)
		C ₁₀	C ₁₂	C ₁₄₊		
1	1	38	59	3	1.15	62
2	2	66	30	4	1.00	54
3	3	45	52	3	1.29	70
4	4	54	41	5	1.05	56
5	5	34	61	5	1.36	73
6	5^d	30	64	6	2.97	124

^aReaction conditions: solvent, toluene (50 mL); pressure 5 atm (1 atm = 101.325 kPa); temperature, 25 °C; time 2 h; amount of catalyst 9.00 μm; Al:Pd, 500; co-catalyst, EtAlCl₂.

^bProduct distribution determined by GC-MS.

^cYield of products determined by the total mass of oligomers produced after the solvent was evaporated.

^dAl:Pd = 1000.

Table 6. Effect of co-catalyst concentration on ethylene oligomerization.^a

Entry	Al:Pd	Oligomers (%) ^b			Yield ^c (g)	TON (kg mol ⁻¹ Pd h ⁻¹)
		C ₁₀	C ₁₂	C ₁₄₊		
1	20	—	—	—	Trace	—
2	50	49	45	6	0.21	10
3	100	57	38	5	0.41	21
4	500	66	30	4	1.00	54
5	1000	65	30	5	1.66	94
6	2000	66	29	5	1.19	64
7	100 ^d	31	65	4	1.79	30
8	500 ^d	38	59	3	1.15	62
9	1000 ^d	50	45	5	2.10	110

^aReaction conditions: solvent, toluene (50 mL); pressure 5 atm (1 atm = 101.325 kPa); temperature, 25 °C; time, 2 h; amount of catalyst, 9.00 μm; co-catalyst, EtAlCl₂; catalyst **2** unless stated otherwise.

^bProduct distribution determined by GC-MS.

^cYield of products determined by the total mass of oligomers produced after the solvent was evaporated.

^dCatalyst **1**.

Fig. 4. The DFT studies (at the B3LYP/6-31+G(*d*) level of theory) of simplified analogues of **L1** (A and B). The more stable conformation is also observed in the solid-state structures of **L1** and **1** (1 cal = 4.184 J).

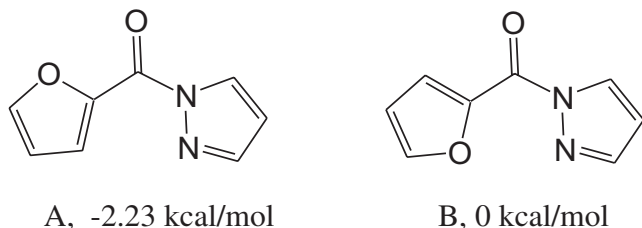
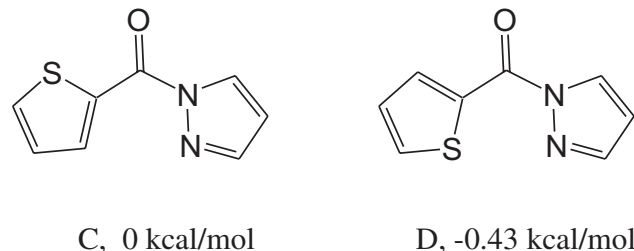


Fig. 5. The DFT studies (at the B3LYP/6-31+G(*d*) level of theory) of simplified analogues of **L2** (C and D). The less stable conformation is observed when **L2** serves as a ligand in **2** (1 cal = 4.184 J).



trend is seen with phosphinidene Pd(II) complexes where prolonged reaction time from 3 to 15 h resulted in reduced oligomer molecular weight from 215 to 180 (18).

An increase in temperature was found to increase the activity of catalyst **1** and a maximum activity was obtained at 60 °C (Table 7). Above 60 °C, the activity of the catalyst dropped (Table 7, entries 8 and 9), usually an indication of catalyst decomposition. This observation is consistent with Pd(II) α -diimine catalysts, which are known to decompose rapidly above 50 °C (21), and that of Guan and Salo (22) that uses bisazaferrocene Pd(II) complexes.

The influence of pressure on ethylene oligomerization is well-established, especially on catalytic activity (21). The ef-

fect of ethylene concentration on oligomerization using catalyst **1** was studied by varying the ethylene pressure from 5 to 35 atm (Table 7, entries 2, 10–12). An increase in ethylene concentration resulted in a significant increase in oligomer yield. We also observed selectivity towards higher oligomers with an increase in pressure (Table 7, entries 2 and 12). For instance, at 5 atm, 71% of C₁₀ and 23% of C₁₂ were produced, respectively, while at 35 atm, 48% of C₁₀ and 41% of C₁₂ were obtained. At high pressures, it has been postulated that ethylene co-oligomerizes with the preformed olefins resulting in a significant increase in oligomer molecular weight (3). A report on bis(salicylaldehyde)nickel catalysed

Table 7. Effect of reaction conditions on ethylene oligomerization.^a

Entry	Temp (°C)	P _{C₂H₄} (atm)	Time (min)	Oligomers (%) ^b			Yield ^c (g)	TON (kg mol ⁻¹ Pd h ⁻¹)
				C ₁₀	C ₁₂	C ₁₄₊		
1	25	5	15	77	20	3	0.28	120
2	25	5	30	71	25	4	0.82	177
3	25	5	60	58	38	4	1.27	137
4	25	5	120	38	59	3	1.30	70
5	25	5	30 ^d	70	24	6	0.93	200
6	25	5	60 ^d	54	41	5	1.40	151
7	40	5	30	36	61	3	1.60	345
8	60	5	30	32	64	4	4.86	1050
9	70	5	30	33	62	5	3.15	680
10	25	10	30	61	36	3	1.00	216
11	25	20	30	51	44	5	1.28	276
12	25	35	30	48	41	11	2.56	542

Note: 1 atm = 101.325 kPa.

^aReaction conditions: solvent, toluene (50 mL); amount of catalyst, 9.00 μm; catalyst **1** used unless stated otherwise; co-catalyst, EtAlCl₂; Al:Pd = 500.

^bProduct distribution determined by GC-MS.

^cYield of products determined by the total mass of oligomers produced after the solvent was evaporated.

^dCatalyst **5**.

ethylene oligomerization found the C₆–C₁₂ yield go up from 23% to 70% when the ethylene pressure was increased from 1 to 20 atm, but the butene content of the oligomerization product dropped from 76% to 30% (23). Our result is in line with this observation, though not as drastic.

Conclusions

Furoyl and thiophene carbonyl pyrazolyl ligands form complexes with palladium(II) that have the same structural motifs as complexes formed by simple substituted pyrazoles with palladium(II). X-ray structures of **1** and **2** confirm that in the solid state of [Pd(L)₂Cl₂] a trans geometry is preferred to cis. Activation of these complexes with the alkyl aluminium compound, EtAlCl₂, results in active catalysts for the oligomerization of ethylene. The major oligomers produced are C₁₀ and C₁₂, and no lower oligomers in the C₄–C₈ range were obtained. This shows that the catalysts favour chain propagation relative to chain termination. The activities of these palladium(II) catalysts are lower compared with the α-diimine Pd(II) complexes, possibly because of the presence of the noncoordinating donor atoms (sulfur and oxygen), which might cause catalyst deactivation by forming adducts with the aluminium co-catalyst. Thermal instability of these catalysts could also contribute to their observed low catalytic activity, as would weakly bound pyrazolyl ligands that could lead to ligand dissociation from the metal centre.

Experimental section

All ligand and complex syntheses were performed under a nitrogen atmosphere using standard Schlenk techniques. All solvents were of analytical grade and were dried and distilled prior to use. Toluene and dichloromethane were dried and distilled from sodium/benzophenone and P₂O₅, respectively. The carbonyl linkers (2-furoyl chloride and 2-thiophene carbonyl chloride) were obtained from Sigma-Aldrich and used as received. The NMR spectra were recorded on a Varian Gemini 2000 instrument (¹H at 200 MHz, ¹³C at

50.3 MHz) at room temperature. The chemical shifts are reported in δ (ppm) and referenced to the residual CHCl₃ in the NMR solvent. Elemental analyses and IR spectroscopy were performed on a Carlo Erba NA analyzer and a PerkinElmer FT-IR Paragon 1000PC, respectively, at the Chemistry Department, University of the Western Cape.

Synthesis of the ligands and complexes

2-(3,5-Dimethylpyrazolyl-1-carbonyl)furan (**L1**)

To a solution of 2-furoyl chloride (2.12 g, 15.60 mmol) in toluene (40 mL) was added 3,5-dimethylpyrazole (1.49 g, 15.60 mmol) and Et₃N (2 mL). The mixture was refluxed for 24 h, filtered to remove the Et₃NHCl by-product, and the solvent removed in vacuo to give a white residue. Purification by column chromatography on silica gel with dichloromethane–hexane (1:1) as the eluent afforded a white solid. Recrystallization from CH₂Cl₂–hexane gave single crystals suitable for X-ray analysis. Yield: 2.52 g (85%). IR (Nujol, cm⁻¹) ν_(C=O): 1702. ¹H NMR (CDCl₃) δ: 2.29 (s, 3H, CH₃, pz), 2.62 (s, 3H, CH₃, pz), 6.02 (s, 1H, pz), 6.61 (dd, 1H, furan, ⁴J_{HH} = 1.6 Hz, ³J_{HH} = 3.6 Hz), 7.71 (dd, 1H, furan, ⁴J_{HH} = 0.8 Hz, ³J_{HH} = 3.6 Hz), 7.94 (dd, 1H, furan, ⁴J_{HH} = 0.8 Hz, ³J_{HH} = 3.8 Hz). ¹³C{¹H} NMR (CDCl₃) δ: 13.2, 13.8, 110.4, 111.7, 123.4, 144.8, 146.9, 152.1, 156.1, 161.8. EI-MS (70 eV) *m/z* (%): 190 (20) [M⁺], 162 (100) [M⁺ – C₂H₄], 95 (40) [M⁺ – C₅N₂H₇], 67 (5) [M⁺ – C₆N₂H₇CO]. Anal. calcd. for C₁₀H₁₀N₂O₂ (%): C 63.25, H 5.32, N 14.71; found: C 62.76, H 4.88, N 14.49.

Compounds **L2–L6** were prepared following the same procedure as described for **L1**.

2-(3,5-Dimethylpyrazolyl-1-carbonyl)thiophene (**L2**)

Compound **L2** was synthesized using 3,5-dimethylpyrazole (1.50 g, 15.60 mmol) and 2-thiophene carbonyl chloride (2.28 g, 15.60 mmol). Yield: 2.41 g (75%). IR (Nujol, cm⁻¹) ν_(C=O): 1675. ¹H NMR (CDCl₃) δ: 2.32 (s, 3H, CH₃, pz), 2.63 (s, 3H, CH₃, pz), 6.03 (s, 1H, pz), 7.15 (dd, 1H, thiophene, ⁴J_{HH} = 1.6 Hz, ³J_{HH} = 4.8 Hz), 7.71 (dd, 1H,

thiophene, $^4J_{\text{HH}} = 1.4$ Hz, $^3J_{\text{HH}} = 4.8$ Hz), 8.34 (d, 1H, thiophene, $^4J_{\text{HH}} = 1.4$ Hz, $^3J_{\text{HH}} = 4.0$ Hz). $^{13}\text{C}\{^1\text{H}\}$ NMR (CDCl_3) δ : 13.3, 14.0, 110.8, 126.4, 127.9, 137.2, 144.5, 151.5, 156.0, 160.0. EI-MS (70 eV) m/z (%): 206 (100) [M^+], 178 (50) [$\text{M}^+ - \text{C}_2\text{H}_4$], 111 (50) [$\text{M}^+ - \text{C}_5\text{N}_2\text{H}_7$], 83 (5) [$\text{M}^+ - \text{C}_6\text{N}_2\text{H}_7\text{CO}$]. Anal. calcd. for $\text{C}_{10}\text{H}_{10}\text{N}_2\text{OS}$ (%): C 58.32, H 4.87, N 13.65; found: C 58.15, H 4.26, N 13.68.

2-(3,5-Di-tert-butylpyrazolyl-1-carbonyl)furan (L3)

Compound **L3** was prepared using 2-furoyl chloride (1.42 g, 10.52 mmol) and 3,5-di-tert-butylpyrazole (2.90 g, 10.52 mmol). Yield: 2.31 g (80%). IR (Nujol, cm^{-1}) $\nu_{(\text{C}=\text{O})}$: 1716. ^1H NMR (CDCl_3) δ : 1.35 (s, 9H, CH_3 , pz), 1.46 (s, 9H, CH_3 , pz), 6.18 (s, 1H, pz), 6.60 (dd, 1H, furan, $^4J_{\text{HH}} = 1.6$ Hz, $^3J_{\text{HH}} = 3.4$ Hz), 7.71 (dd, 1H, furan, $^4J_{\text{HH}} = 0.8$ Hz, $^3J_{\text{HH}} = 1.6$ Hz), 7.82 (dd, 1H, furan, $^4J_{\text{HH}} = 0.8$ Hz, $^3J_{\text{HH}} = 3.8$ Hz). $^{13}\text{C}\{^1\text{H}\}$ NMR (CDCl_3) δ : 29.0, 29.3, 31.9, 32.8, 105.5, 111.7, 123.1, 146.5, 156.1, 158.0, 161.6. EI-MS (70 eV) m/z (%): 274 (45) [M^+], 244 (30) [$\text{M}^+ - \text{C}_2\text{H}_6$], 232 (100) [$\text{M}^+ - \text{C}_3\text{H}_6$], 217 (95) [$\text{M}^+ - \text{C}_{11}\text{N}_2\text{H}_{19}$], 67 (5) [$\text{M}^+ - \text{C}_{11}\text{N}_2\text{H}_{19}\text{CO}$]. Anal. calcd. for $\text{C}_{16}\text{H}_{22}\text{N}_2\text{O}_2$ (%): C 69.82, H 8.36, N 10.18; found: C 69.77, H 8.26, N 10.02.

2-(3,5-Di-tert-butylpyrazolyl-1-carbonyl)thiophene (L4)

Compound **L4** was prepared by reacting 3,5-di-tert-butylpyrazole (1.82 g, 10.34 mmol) with 2-thiophene carbonyl chloride (1.37 g, 9.35 mmol). Yield: 1.50 g (52%). IR (Nujol, cm^{-1}) $\nu_{(\text{C}=\text{O})}$: 1686. ^1H NMR (CDCl_3) δ : 1.37 (s, 9H, CH_3 , pz), 1.46 (s, 9H, CH_3 , pz), 6.17 (s, 1H, pz), 7.12 (dd, 1H, thiophene, $^4J_{\text{HH}} = 1.8$ Hz, $^3J_{\text{HH}} = 5.2$ Hz), 7.71 (dd, 1H, thiophene, $^4J_{\text{HH}} = 1.4$ Hz, $^3J_{\text{HH}} = 5.2$ Hz), 8.83 (dd, 1H, thiophene, $^4J_{\text{HH}} = 1.6$ Hz, $^3J_{\text{HH}} = 4.0$ Hz). $^{13}\text{C}\{^1\text{H}\}$ NMR (CDCl_3) δ : 28.9, 29.4, 32.1, 32.8, 106.0, 125.8, 137.2, 157.4, 159.7, 169.8. EI-MS (70 eV) m/z (%): 290 (63) [M^+], 275 (20) [$\text{M}^+ - \text{CH}_3$], 233 (65) [$\text{M}^+ - \text{C}_4\text{H}_9$], 191 (30) [$\text{M}^+ - \text{C}_7\text{H}_{15}$], 111 (100) [$\text{M}^+ - \text{C}_{11}\text{N}_2\text{H}_{19}$], 83 (5) [$\text{M}^+ - \text{C}_{11}\text{N}_2\text{H}_{19}\text{CO}$]. Anal. calcd. for $\text{C}_{16}\text{H}_{22}\text{N}_2\text{OS}$ (%): C 65.98, H 7.90, N 9.62; found: C 65.86, H 8.32, N 9.34.

2-(3,5-Diphenylpyrazolyl-1-carbonyl)thiophene (L5)

Compound **L5** was synthesized by reacting 2-thiophene carbonyl chloride (1.73 g, 11.85 mmol) and 3,5-diphenylpyrazole (2.61 g, 11.86 mmol). Yield: 3.07 g (75%). IR (Nujol, cm^{-1}) $\nu_{(\text{C}=\text{O})}$: 1689. ^1H NMR δ : 6.61 (s, 1H, pz), 6.98 (d, 1H, thiophene, $^3J_{\text{HH}} = 3.6$ Hz), 7.32 (m, 8H, ph), 7.63 (d, 1H, thiophene, $^3J_{\text{HH}} = 3.8$ Hz), 7.82 (m, 2H, ph), 8.14 (d, 1H, thiophene, $^3J_{\text{HH}} = 3.8$ Hz). $^{13}\text{C}\{^1\text{H}\}$ NMR (CDCl_3) δ : 109.2, 125.9, 126.5, 127.5, 128.3, 128.8, 130.6, 131.2, 133.0, 137.1, 137.9, 147.8, 153.1, 159.2. EI-MS (70 eV) m/z (%): 330 (100) [M^+], 302 (85) [$\text{M}^+ - \text{C}_2\text{H}_4$], 189 (20) [$\text{M}^+ - \text{C}_{13}\text{H}_9$], 111 (85) [$\text{M}^+ - \text{C}_{15}\text{H}_{11}\text{N}_2$], 83 (4) [$\text{M}^+ - \text{C}_{15}\text{H}_{11}\text{N}_2\text{CO}$]. Anal. calcd. for $\text{C}_{20}\text{H}_{14}\text{N}_2\text{OS}$ (%): C 72.70, H 4.27, N 8.48; found: C 72.68, H 4.05, N 8.36.

2-(Pyrazolyl-1-carbonyl) furan (L6)

Compound **L6** was prepared by reacting 2-furoyl chloride (2.97 g, 22.12 mmol) and unsubstituted pyrazole (1.50 g, 22.00 mmol). Yield: 2.40 g (75%). IR (Nujol, cm^{-1}) $\nu_{(\text{C}=\text{O})}$: 1685. ^1H NMR (CDCl_3) δ : 6.50 (dd, 1H, pz, $^4J_{\text{HH}} = 1.4$ Hz, $^3J_{\text{HH}} = 3.0$ Hz), 6.65 (dd, 1H, furan, $^4J_{\text{HH}} = 1.8$ Hz, $^3J_{\text{HH}} = 3.6$ Hz), 7.78 (dd, 2H, pz, $^4J_{\text{HH}} = 1.6$ Hz, $^3J_{\text{HH}} = 3.8$ Hz),

8.08 (dd, 1H, furan, $^4J_{\text{HH}} = 0.8$ Hz, $^3J_{\text{HH}} = 3.8$ Hz), 8.44 (dd, 1H, furan, $^4J_{\text{HH}} = 0.8$ Hz, $^3J_{\text{HH}} = 3.8$ Hz). $^{13}\text{C}\{^1\text{H}\}$ NMR (CDCl_3) δ : 111.4, 117.4, 124.3, 132.6, 144.9, 145.9, 147.8, 161.8. EI-MS (70 eV) m/z (%): 162 (100) [M^+], 134 (100) [$\text{M}^+ - \text{CN}_2\text{H}_2$], 95 (40) [$\text{M}^+ - \text{C}_3\text{N}_2\text{H}_3$], 67 (5) [$\text{M}^+ - \text{C}_3\text{N}_2\text{H}_3\text{CO}$]. Anal. calcd. for $\text{C}_8\text{H}_6\text{N}_2\text{O}_2$ (%): C 59.32, H 3.72, N 17.34; found: C 58.89, H 3.35, N 16.81.

Dichloro{bis-2-(3,5-dimethylpyrazolyl-1-carbonyl)furan}palladium(II) (1)

To a solution of $[\text{Pd}(\text{NCMe})_2\text{Cl}_2]$ (0.20 g, 0.68 mmol) in dichloromethane (20 mL) was added **L1** (0.26 g, 1.43 mmol). The mixture was stirred at room temperature for 6 h and the resultant solution was concentrated in vacuo to about 10 mL. An analytically pure yellow powder was obtained upon addition of an equal volume of hexane. Yield: 0.28 g (79%). IR (Nujol, cm^{-1}) $\nu_{(\text{C}=\text{O})}$: 1694. ^1H NMR (CDCl_3) δ : 2.34 (s, 6H, CH_3 , pz), 2.44 (s, 6H, CH_3 , pz), 6.03 (s, 2H, pz), 6.77 (d, 2H, furan, $^3J_{\text{HH}} = 3.6$ Hz), 7.70 (d, 2H, furan, $^3J_{\text{HH}} = 3.6$ Hz), 7.91 (d, 2H, furan, $^3J_{\text{HH}} = 3.6$ Hz). $^{13}\text{C}\{^1\text{H}\}$ NMR (CDCl_3) δ : 12.8, 15.1, 110.9, 113.3, 126.8, 146.1, 147.1, 149.4, 154.8, 155.9. Anal. calcd. for $\text{C}_{20}\text{H}_{20}\text{N}_4\text{O}_4\text{PdCl}_2$ (%): C 43.09, H 3.59, N 10.05; found: C 42.57, H 3.20, N 9.65.

Complexes **2–4** and **6** were prepared in a similar manner as described for **1**.

Dichloro{bis-2-(3,5-dimethylpyrazolyl-1-carbonyl)thiophene}palladium(II) (2)

Complex **2** was prepared using ligand **L2** (0.50 g, 3.42 mmol) and $[\text{PdCl}_2(\text{NCMe})_2]$ (0.45 g, 1.71 mmol). Recrystallization from dichloromethane–hexane gave yellow single crystals suitable for X-ray analysis. Yield: 0.61 g (62%). IR (Nujol, cm^{-1}) $\nu_{(\text{C}=\text{O})}$: 1688. ^1H NMR (CDCl_3) δ : 2.30 (s, 6H, CH_3 , pz), 2.32 (s, 6H, CH_3 , pz), 6.00 (s, 2H, pz), 7.29 (dd, 2H, thiophene, $^4J_{\text{HH}} = 1.6$ Hz, $^3J_{\text{HH}} = 3.8$ Hz), 7.73 (dd, 2H, thiophene, $^4J_{\text{HH}} = 1.6$ Hz, $^3J_{\text{HH}} = 3.8$ Hz), 8.02 (dd, 2H, thiophene, $^4J_{\text{HH}} = 6$ Hz, $^3J_{\text{HH}} = 3.8$ Hz). $^{13}\text{C}\{^1\text{H}\}$ NMR (CDCl_3) δ : 12.6, 14.4, 110.1, 126.4, 128.4, 136.2, 136.5, 140.1, 146.1, 155.2, 160.0. Anal. calcd. for $\text{C}_{20}\text{H}_{20}\text{N}_4\text{O}_2\text{S}_2\text{PdCl}_2$ (%): C 40.83, H 3.43, N 9.51; found: C 40.84, H 2.69, N 9.53.

Dichloro{bis-2-(3,5-di-tert-butylpyrazolyl-1-carbonyl)furan}palladium(II) (3)

Complex **3** was prepared using ligand **L3** (0.37 g, 1.35 mmol) and $[\text{Pd}(\text{NCMe})_2\text{Cl}_2]$ (0.18 g, 0.68 mmol). Yield: 0.25 g (52%). IR (Nujol, cm^{-1}) $\nu_{(\text{C}=\text{O})}$: 1705. ^1H NMR (CDCl_3) δ : 1.32 (s, 18H, CH_3 , pz), 1.46 (s, 18H, CH_3 , pz), 6.17 (s, 2H, pz), 6.58 (dd, 2H, furan, $^4J_{\text{HH}} = 1.7$ Hz, $^3J_{\text{HH}} = 3.6$ Hz), 7.71 (dd, 2H, furan, $^4J_{\text{HH}} = 1.8$ Hz, $^3J_{\text{HH}} = 3.4$ Hz), 7.82 (dd, 2H, furan, $^4J_{\text{HH}} = 1.8$ Hz, $^3J_{\text{HH}} = 3.4$ Hz). $^{13}\text{C}\{^1\text{H}\}$ NMR (CDCl_3) δ : 28.8, 29.7, 30.5, 31.6, 100.1, 111.7, 119.3, 125.8, 137.2, 146.7, 156.1, 157.8. Anal. calcd. for $\text{C}_{34}\text{H}_{50}\text{N}_4\text{O}_4\text{PdCl}_2 \cdot 2\text{CH}_2\text{Cl}_2$ (%): C 45.53, H 5.58, N 6.25; found: C 46.05, H 5.03, N 6.55.

Dichloro{bis-2-(3,5-di-tert-butylpyrazolyl-1-carbonyl)thiophene}palladium(II) (4)

Complex **4** was prepared using ligand **L4** (0.44 g, 1.52 mmol) and $[\text{Pd}(\text{NCMe})_2\text{Cl}_2]$ (0.20 g, 0.76 mmol). Yield: 0.32 g (58%). IR (Nujol, cm^{-1}) $\nu_{(\text{C}=\text{O})}$: 1694. ^1H NMR

(CDCl₃) δ : 1.32 (s, 18H, CH₃, pz), 1.46 (s, 18H, CH₃, pz), 6.19 (s, 2H, pz), 7.13 (dd, 2H, thiophene, ⁴J_{HH} = 1.6 Hz, ³J_{HH} = 5.0 Hz), 7.72 (dd, 2H, thiophene, ⁴J_{HH} = 1.2 Hz, ³J_{HH} = 5.4 Hz), 8.26 (dd, 2H, thiophene, ⁴J_{HH} = 1.6 Hz, ³J_{HH} = 4.2 Hz). Anal. calcd. for C₃₂H₄₆N₂O₂S₂PdCl₂ (%): C 49.05, H 6.27, N 7.63; found: C 48.75, H 5.06, N 7.66.

Dichloro{bis-2-(3,5-diphenylpyrazolyl-1-carbonyl)thiophene}palladium(II) (5)

Complex **5** was synthesized by reacting **L5** (0.50 g, 1.53 mmol) and [Pd(NCMe)₂Cl₂] (0.20 g, 0.77 mmol). Yield: 0.23 g (37%). IR (Nujol, cm⁻¹) $\nu_{(C=O)}$: 1694. ¹H NMR (CDCl₃) δ : 7.20 (s, 1H, pz), 7.46 (d, 1H, thiophene, ³J_{HH} = 4.0 Hz), 8.16 (m, 10H, benzene), 8.37 (d, 1H, thiophene, ³J_{HH} = 3.6 Hz), 8.42 (d, 1H, thiophene, ³J_{HH} = 3.8 Hz). ¹³C{¹H} NMR (CDCl₃) δ : 109.2, 125.9, 126.5, 127.5, 127.7, 128.4, 128.7, 130.5, 131.2, 133.0, 137.0, 137.9, 147.8, 153.1, 158.2. Anal. calcd. for C₄₀H₂₈N₂O₂S₂PdCl₂ (%): C 57.32, H 4.37, N 6.63; found: C 56.82, H 4.15, N 6.16.

Dichloro{bis-2-(pyrazolyl-1-carbonyl)furan}palladium(II) (6)

To a solution of compound **L6** (0.80, 4.94 mmol) in dichloromethane (30 mL), [Pd(NCMe)₂Cl₂] (0.63 g, 2.47 mmol) was added. A light brown precipitate formed immediately. The resultant mixture was stirred for 3 h, filtered, and the yellow solid dried. Yield: 1.01 g (80%). IR (Nujol, cm⁻¹) $\nu_{(C=O)}$: 1712. ¹H NMR (DMSO-*d*₆) δ : 6.64 (dd, 2H, pz, ⁴J_{HH} = 1.6 Hz, ³J_{HH} = 3.0 Hz), 6.78 (dd, 2H, furan, ⁴J_{HH} = 1.6 Hz, ³J_{HH} = 3.6 Hz), 7.79 (dd, 4H, pz, ⁴J_{HH} = 0.8 Hz, ³J_{HH} = 3.6 Hz), 8.15 (dd, 2H, furan, ⁴J_{HH} = 0.8 Hz, ³J_{HH} = 3.0 Hz), 8.52 (dd, 2H, furan, ⁴J_{HH} = 0.8 Hz, ³J_{HH} = 1.8 Hz). ¹³C{¹H} NMR (CDCl₃) δ : 106.4, 110.1, 112.2, 113.2, 117.8, 125.0, 130.5, 145.3, 147.1, 149.8, 154.3, 159.4. Anal. calcd. for C₁₆H₁₂N₄O₄PdCl₂ (%): C 38.31, H 2.41, N 11.17; found: C 38.06, H 2.30, N 10.33.

Ethylene oligomerization

Ethylene oligomerization was performed in a 300 mL stainless steel autoclave loaded with the respective catalyst and the appropriate amount EtAlCl₂ as the co-catalyst. This was carried out in a nitrogen-purged glovebox. The general procedure involved charging the autoclave with a palladium complex and EtAlCl₂ (25% in toluene) in 100 mL of dry toluene. The Al:Pd ratio used was between 20–2000. The autoclave was sealed, removed from the glovebox and loaded into the reactor chamber. The autoclave was flushed three times with ethylene and heated to the required temperature. The desired ethylene pressure was set and a constant flow of ethylene was maintained throughout the reaction. At the end of the reaction, an aliquot of the reaction mixture was taken for the GC analysis. The reaction was quenched by the addition of ethanol after which the solvent was removed in vacuo and the mass of the total nonvolatile products determined. Analysis of the oligomers was performed using a Finnigan-MAT GCQ GC-MS, equipped with an electron impact ion-

ization source at 70 eV and a 30 m HP PONA capillary column with a stationary phase based on 5% poly(methylphenylsiloxane). The rate of increase in oven temperature of the GC was set at 20 °C min⁻¹ and then increased by 10 °C min⁻¹ until a temperature of 260 °C was reached. Under these conditions, it was possible to separate C₄ to C₂₀ olefins. The retention times of the individual components were determined using standard samples of each olefin. Quantitative analysis of the olefins was done by the internal standard reference method using pentadecane as the internal reference.

X-ray crystallography

Crystal evaluation and data collection for **L1**, **1**, and **2** were performed on a Bruker CCD-1000 diffractometer with Mo K α (λ = 0.710 73 Å) radiation and the diffractometer to crystal distance of 4.9 cm. The initial cell constants were obtained from three series of ω scans at different starting angles. The reflections were successfully indexed by an automated indexing routine built in the SMART program. The absorption correction was based on fitting a function to the empirical transmission surface as sampled by multiple equivalent measurements (24). The structures were solved by direct methods and refined by least-squares techniques using the SHELXTL program (24). All non-hydrogen atoms were refined with anisotropic displacement coefficients. All hydrogen atoms were included in the structure factor calculation at idealized positions and were allowed to ride on the neighbouring atoms with relative isotropic displacement coefficients. Additional crystallographic data for the structures are deposited with the Cambridge Crystallographic Data Centre as supplementary publication numbers CCDC 257819 (**L1**), CCDC 257820 (**1**), and CCDC 257818 (**2**).⁴

Acknowledgements

Financial support by the National Research Foundation (NRF) South Africa is highly appreciated. We thank Professor Len Barbour, University of Stellenbosch, South Africa, for solving the structure of compound **2** as a service.

References

- (a) S. Trofimenko. *Prog. Inorg. Chem.* **34**, 115 (1986); (b) S. Trofimenko. *Chem. Rev.* **72**, 497 (1972); (c) Y. Sun, X. Chen, P. Cheng, S. Yan, D. Zheng Liao, and P. Wen Shen. *J. Mol. Struct.* **597**, 191 (2001).
- (a) R. Mukherjee. *Coord. Chem. Rev.* **203**, 166 (2000); (b) S. Mecking. *Coord. Chem. Rev.* **203**, 325 (2000); (c) S. Trofimenko. *Chem. Rev.* **93**, 943 (1993).
- (a) J. Skupinska. *Chem. Rev.* **91**, 613 (1991); (b) M. Peuckert, W. Keim, S. Storp, and S.R. Weber. *J. Mol. Catal.* **20**, 115 (1983).
- W. Keim. *J. Mol. Catal.* **52**, 19 (1989).
- (a) C.M. Killian, L.K. Johnson, and M. Brookhart. *Organometallics*, **16**, 2005 (1997); (b) L.K. Johnson, C.M. Killian, and M. Brookhart. *J. Am. Chem. Soc.* **117**, 6414 (1995);

⁴Supplementary data for this article are available on the Web site or may be purchased from the Depository of Unpublished Data, Document Delivery, CISTI, National Research Council Canada, Ottawa, ON K1A 0S2, Canada. DUD 3687. For more information on obtaining material refer to http://cisti-icist.nrc-cnrc.gc.ca/irm/unpub_e.shtml. CCDC 257818–257820 contain the crystallographic data for this manuscript. These data can be obtained, free of charge, via www.ccdc.cam.ac.uk/conts/retrieving.html (Or from the Cambridge Crystallographic Data Centre, 12 Union Road, Cambridge CB2 1EZ, UK; fax +44 1223 336033; or deposit@ccdc.cam.ac.uk).

- (c) S.A. Svejda, L.K. Johnson, and M. Brookhart. *J. Am. Chem. Soc.* **121**, 10 634 (1999).
- G.J.P. Britovsek, S.P.D. Baugh, V.C. Gibson, and D.F. Wass. *Angew. Chem. Int. Ed.* **38**, 428 (1999).
 - B.L. Small and M. Brookhart. *J. Am. Chem. Soc.* **120**, 7143 (1998).
 - S. Tsuji, T.R. Younkin, D.C. Swenson, and R.F. Jordan. *Organometallics*, **18**, 4758 (1998).
 - (a) K. Li, J. Darkwa, I.A. Guzei, and S.F. Mapolie. *J. Organomet. Chem.* **660**, 108 (2002); (b) S.M. Nelana, J. Darkwa, I.A. Guzei, and S.F. Mapolie. *J. Organomet. Chem.* **689**, 1835 (2004).
 - I.A. Guzei, K. Li, G.A. Bikzhanova, J. Darkwa, and S.F. Mapolie. *Dalton Trans.* 715 (2003).
 - L.K. Johnson, S. Mecking, and M. Brookhart. *J. Am. Chem. Soc.* **118**, 11 664 (1998).
 - (a) I.A. Guzei and M. Wendt. SOLID-G [computer program]. Madison, Wis. 2004; (b) I.A. Guzei. *In* 2004 Annual Meeting of the American Crystallographic Association, 17–22 July 2004, Chicago.
 - W. Kemp. *Organic spectroscopy*. 3rd ed. Macmillan Education Ltd., London. 1991. p. 36.
 - I.A. Guzei, K. Li, and J. Darkwa. *J. Chem. Crystallogr.* **35**, 197 (2005).
 - F.H. Allen. *Acta Crystallogr. Sect. B*, **B58**, 380 (2002).
 - M.J. Frisch, G.W. Trucks, H.B. Schlegel, G.E. Scuseria, M.A. Robb, J.R. Cheeseman, V.G. Zakrzewski, J.A. Montgomery, Jr., R.E. Stratmann, J.C. Burant, S. Dapprich, J.M. Millam, A.D. Daniels, K.N. Kudin, M.C. Strain, O. Farkas, J. Tomasi, V. Barone, M. Cossi, R. Cammi, B. Mennucci, C. Pomelli, C. Adamo, S. Clifford, J. Ochterski, G.A. Petersson, P.Y. Ayala, Q. Cui, K. Morokuma, D.K. Malick, A.D. Rabuck, K. Raghavachari, J.B. Foresman, J. Cioslowski, J.V. Ortiz, A.G. Baboul, B.B. Stefanov, G. Liu, A. Liashenko, P. Piskorz, I. Komaromi, R. Gomperts, R.L. Martin, D.J. Fox, T. Keith, M.A. Al-Laham, C.Y. Peng, A. Nanayakkara, M. Challacombe, P.M.W. Gill, B. Johnson, W. Chen, M.W. Wong, J.L. Andres, C. Gonzalez, M. Head-Gordon, E.S. Replogle, and J.A. Pople. GAUSSIAN98. Revision A9 [computer program]. Gaussian Inc., Pittsburgh, Pennsylvania. 1998.
 - Z. Guan and W.J. Marshall. *Organometallics*, **21**, 3580 (2002).
 - O. Daugulis, M. Brookhart, and P.S. White. *Organometallics*, **21**, 5935 (2002).
 - F. Speiser, P. Braunstein, L. Saussine, and R. Welter. *Inorg. Chem.* **43**, 1649 (2004).
 - J.M. Malinoski and M. Brookhart. *Organometallics*, **22**, 5324 (2003).
 - S.D. Ittel, M. Brookhart, and L.K. Johnson. *Chem. Rev.* **100**, 1169 (2000).
 - Z. Guan and E.V. Salo. *Organometallics*, **22**, 5033 (2003).
 - C. Carlini, M. Isola, V. Liuzzo, A.M.R. Galletti, and G. Sbrana. *Appl. Catal. A*, **231**, 307 (2002).
 - Bruker-AXS SADABS. Version 2.05 software reference manual. Bruker-AXS, Madison, Wisconsin. 2000–2004; Bruker-AXS SAINT. Version 6.22 software reference manual. Bruker-AXS, Madison, Wisconsin. 2000–2004; Bruker-AXS SHELXTL. Version 6.10 software reference manual. Bruker-AXS, Madison, Wisconsin. 2000–2004; Bruker-AXS SMART 5.622 software reference manual. Bruker-AXS, Madison, Wisconsin. 2000–2004.